Penerbit Akademia Baru

Journal of Advanced Research in Micro and Nano Engineering

Journal homepage:
https://www.akademiabaru.com/submit/index.php/armne/index
ISSN: 2756-8210

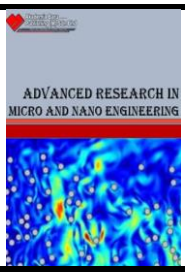

Vanadium Aluminium Carbide Saturable Absorber in Passively Q-switched Erbium-doped Fibre Laser

Wei Ling Ooi[1], Azura Hamzah[1,*], Muhammad Amir Fikri Asraf[1], Kawther M. Musthafa[1], Ahmad Haziq Aiman Rosol[1]

[1] Malaysia-Japan International Institute of Technology, Universiti Teknologi Malaysia,54100 Kuala Lumpur, Malaysia

ARTICLE INFO

Article history:
Received 19 April 2024
Received in revised form 29 May 2024
Accepted 18 July 2024
Available online 31 August 2024

Keywords:
Saturable absorber (SA); Q-switched; MAX phases; vanadium aluminium carbide (V_4AlC_3); erbium-doped fibre laser (EDFL)

ABSTRACT

Following the success of graphene saturable absorber (SA) in the development of passively Q-switched fibre lasers within the past decade, research on two-dimensional (2-D) nanomaterials SAs have shown a significant rise in demands. Nonetheless, there have been several unavoidable setbacks due to the nature of certain nanomaterials, in terms of optical, electronic and physical properties up until the reveal of transition metal carbide (MXene) nanomaterials. These metal-ceramic materials exhibit excellent optical and electrical properties as well as outstanding physical characteristics. However, their synthesis processes involve hazardous and highly acidic chemicals, which drove the researchers to adopt their precursors— ternary nanolaminate carbides (MAX phases) nanomaterials with a simpler and more exquisite fabrication process. This paper presents a passively Q-switched erbium-doped fibre laser (EDFL) with the utilisation of a MAX phases nanomaterial, vanadium aluminium carbide (V_4AlC_3) as SA. The V_4AlC_3 SA was fabricated through the solution casting technique with polyvinyl alcohol as the host polymer. The V_4AlC_3 SA was then integrated into a passively Q-switched EDFL configuration. The performance of V_4AlC_3 SA as a Q-switcher was determined with the assistance of an optical spectrum analyser (OSA), mixed domain oscilloscope (MDO), and optical power meter (OPM). The maximum pulse repetition rate and minimum pulse width were 54.37 kHz and 6.43 μs, respectively. The minimum repetition interval was 18.33 μs and the duty cycle was 0.326. The highest attained output power was 2.5 mW. Through calculation, the maximum pulse energy and peak power were identified as 45.246 nJ and 6.602 mW. The extensively gigantic pulses in nanosecond duration at 1560.16 nm was accomplished by the V_4AlC_3 SA, thus proving its stability which also signifies good applications especially those acquiring stable high power and energy.

1. Introduction

The great demand for pulsed lasers nowadays is owing to their excellent non-linear effects and intensive power density in short pulse duration [1,2]. Compared to conventional continuous-wave (CW) lasers, pulsed lasers have precise and eye-safe responses and outstanding thermal withstand

* *Corresponding author.*
E-mail address: azurahamzah@utm.my

https://doi.org/10.37934/armne.22.1.4355

[3,4]. Correspondingly, pulsed fibre lasers are preferable among the types of lasers because of the nature of fibre optics itself; i.e. compact size, low signal attenuation, and immunity to electromagnetic and radio frequency interference [5,6]. In short, pulsed fibre lasers provide top-quality optical pulses with high-power density and fast duration with minimal loss.

In general, pulsed fibre lasers are classified into Q-switched and mode-locked [7]. Q-switched fibre lasers have intensive power intensity in short pulse duration, whereas mode-locked fibre lasers possess lower power density but ultrafast pulse duration [8,9]. Both offer distinct benefits for various requisites. These can be attained through active and passive approaches [10]. The passive approach, which utilises saturable absorbers (SAs) to modulate the Q-factor has been favoured over the active approach, which involves external modulators [11]. The SAs are the alternative solution as they present low-cost fabrication and a simple framework to construct an all-fibred environment for overcoming disturbances and interferences [12].

The recent research on passively Q-switched fibre lasers is concentrated on the material selection of the SAs [13-15]. The standards of the material selection of SAs are centred on their stability, nonlinearity, response and relaxation time, modulation depth, operational wavelength range, and damage threshold [16]. Semiconductor saturable absorber mirrors (SESAMs) have been the most reliable and popularised SAs in the past two decades [17]. SESAMs are advantaged by their exceptional saturation fluence, modulation depth, endurance, operational wavelength coverage, and recovery time [18]. Notwithstanding, these dominances are constrained by the expensive price and complexity of their manufacturing, inadequate damage threshold, appropriateness of semiconductor materials and temperature stability [19-21].

Consequently, low-dimensional nanomaterials, particularly two-dimensional (2-D) nanomaterials with prominent optical and electronic properties are good to perform as SAs [13]. The superiority of 2-D nanomaterials is because their excessive wideband absorptions make them sufficient for various applications [22]. They exhibit impressive saturation recovery rates, ultrafast electron mobility, and remarkably high damage threshold contributing to the energetic giant Q-switching pulses [23]. Furthermore, the straightforward production of 2-D nanomaterial SAs also streamlined and commercialised the fibre laser [13].

The accomplishment of graphene SAs in 2009 unlocked the implementation of 2-D nanomaterials, specifically, topological insulators (TIs), transition metal dichalcogenides (TMDs), black phosphorus (BP), bismuthene, antimonene, and transition metal carbide/nitrides/carbonitrides (MXenes) [24-29]. These nanomaterials yield excellent non-linear properties due to their atomic bonding and layer-intensity dependence [22]. All things considered, there are still several unavoidable issues that remain to be addressed. To be specific, this pertains to graphene with relatively low modulation depth, and weak light-matter interaction although it exhibits excellently wide operational wavelength, high damage threshold and fast response time [30,31].

Other 2-D SAs are also inflicted with various problems on the grounds of their natures and characteristics. For example, TIs have weak stability due to temperature and humidity factors besides their limited operational wavelength coverage; the fabrication and the utilisation of TMD SAs are affected by their lower saturation fluences; BP SA, bismuthine SA and antimonene SA that oxidise easily not only faced problems in quality management but need more expenses and processes in its protection [32-35].

MXene SAs are some of the options for solving these problems. In 2017, the first employment of MXene nanomaterial SA, titanium carbonitrides (Ti_3CN) in a Q-switched fibre laser at 2.0 μm region was reported by Jhon *et al.,* [36]. The metal-ceramic combination of MXene SAs manifests remarkable linear and non-linear optical absorption, electrical and thermal conductivity, high damage threshold, great melting point, corrosive resistance and outstanding stiffness and elasticity

[37,38]. In addition to that, vanadium carbide (V_4C_3) gained attention due to its significant wide operational wavelength coverage and outstanding non-linear absorption reported by Lee *et al.,* in 2023 [39]. This is further reinforced when Qin *et al.,* reported that V_4C_3 has advantages in their electronic and physical properties, specifically, electrical conductivity, melting point, mechanical modulus, hardness, friction coefficient, and corrosion resistance to withstand environmental factors [40].

The utilisation of V_4C_3 SA is restrained by its preparation as an etching process is essential to produce V_4C_3. This process is complicated because it needs a combination of high-acidic solutions to etch the V_4C_3 from its parent material, vanadium aluminium carbide (V_4AlC_3) [41]. On the flip side, there has been research on the parent materials of MXene nanomaterials, which are the ternary nanolaminates carbides (MAX phases), which were introduced by Ahmad *et al.,* and *Lee et al.,* who use the assortment of titanium aluminium carbide (Ti_3AlC_2 and Ti_2AlC respectively) in 2019 [42,43]. This benchmarked the direct utilisation of V_4AlC_3 SA in passively Q-switched fibre laser configuration.

This paper presents the implementation of V_4AlC_3 SA as a Q-switcher in an erbium-doped fibre laser (EDFL) at the 1.5 μm region. Initiated from the preface, the fabrication of V_4AlC_3 SA was achieved via the solution casting technique by using polyvinyl alcohol (PVA) solution as the host polymer. The fabricated V_4AlC_3 SA was then integrated into the Q-switched EDFL ring cavity for SA significance determination and Q-switching parameters analysis. The significance of V_4AlC_3 SA was identified through the observation of centre wavelength shifting of the fibre laser configuration with and without the V_4AlC_3 SA. The temporal parameters, which are the pulse repetition rate, pulse repetition interval, pulse width and duty cycle and power-related parameters, which are output power, pulse energy and peak power were analysed along with the increasing pump power.

2. Methodology

In this section, the fabrication of V_4AlC_3 SA, the pump characterisation of the laser diode and the passively Q-switched EDFL ring cavity configuration will be discussed.

2.1 Fabrication of V_4AlC_3 SA

Figure 1 illustrates the fabrication of V_4AlC_3 SA through the solution casting technique. This technique is a straightforward and affordable method to fabricate high-quality SAs by using a host polymer to adjoin the particles of V_4AlC_3. PVA solution effectively functions as a host polymer as it is odourless, colourless and eco-friendly [44,45]. In 2020, Ahmad *et al.,* reported that PVA is a good host polymer that does not modify the Q-switching effect of the material itself [46]. Hence, this fabrication employed a PVA solution as the host polymer to adhere the V_4AlC_3 particles to form a functional SA thin film. This procedure can be mainly divided into three parts, the preparation of PVA solution, the preparation of V_4AlC_3 solution and the combination of them.

Initiated with the preparation of PVA, 1 g of PVA powder was put on the electronic balance (OHAUS, AX224/E). 120 ml of pure deionised (DI) water was mixed with the weighed PVA powder and stirred by a hot plate stirrer (THERMO FISHER SCIENTIFIC, SP88857200). The stirring process was carried out for 24 hours with a stirring speed of 300 rpm and a hot-plate temperature of 200 °C. The V_4AlC_3 bulky powder was measured and mixed up with 100 ml DI water. The stirring speed was fixed at 300 rpm while the temperature of the hot plate was adjusted to 25 °C for this 48-hour stirring procedure. 1.5 ml of PVA solution and 1.5 ml were extracted and poured into another clean beaker. The mixture is located and stirred on the hot plate stirrer. This process was held for 24 hours with 300 rpm stirring speed at room temperature.

The perfectly stirred V_4AlC_3-PVA solution was sonicated with a bath sonicator ((FISHERBRAND, FB15050). This process took 2 hours to apply the sound energy of an average frequency of 30 kHz to agitate the mixture for its firm distribution. The V_4AlC_3-PVA solution was then poured into a dirt-free 5-ml petri dish cleaned with alcohol. The petri dish was situated in a dry and sterilised environment at room temperature. The V_4AlC_3-PVA solution in a petri dish was left to dry naturally for at least 72 hours. The completely solidified V_4AlC_3 SA thin film was then peeled off from the petri dish. Hence, a V_4AlC_3 SA with a 30 mm diameter was obtained. The V_4AlC_3 SA was then cut into approximately 1 mm size for incorporation into the Q-switched EDFL ring cavity configuration by applying optical indexing gel.

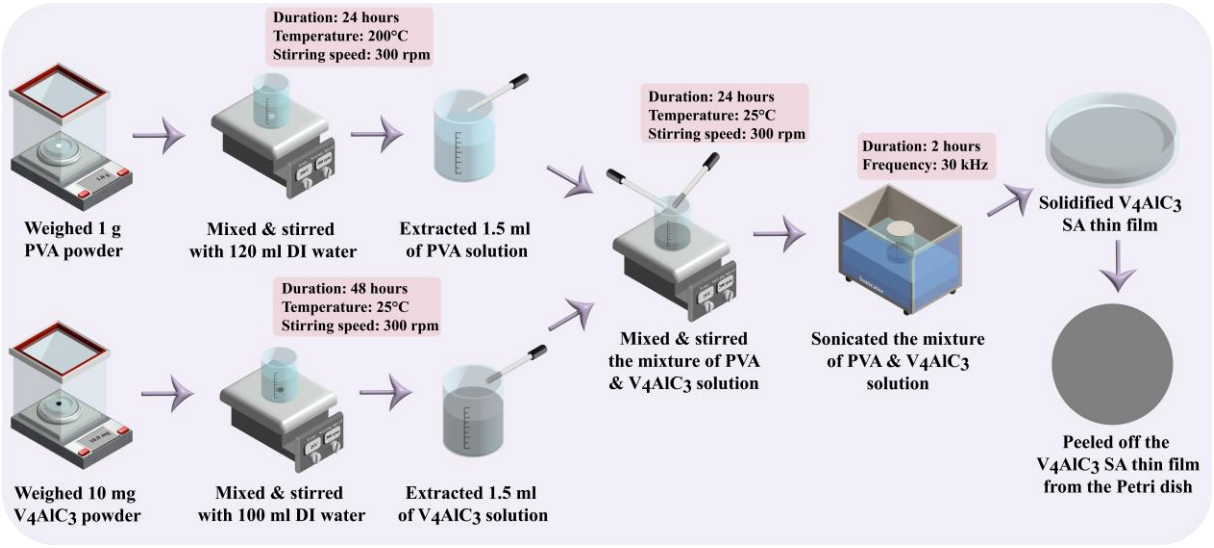

Fig. 1. Fabrication of V_4AlC_3 SA thin film through solution casting technique

2.2 Pump Characterisation of the Laser Diode

The pump characterisation of the laser diode (LD) was done before its utilisation as a pumping power source to ensure its functionality. Figure 2 shows the setup configuration of the pump characterisation of LD. A 980 nm LD (Q-photonics, QFLD-405-20S) in the benchtop laser controller (GOOCH & HOUSEGO, EM595) is the characterised intention. It is connected to the 980 nm end of the 980/1550 nm wavelength division multiplexer (THORLABS, WDM 980/1550 nm) while the 1550 nm end is connected to the optical power meter (OPM; Thorlabs, PM100D). The pump power ranges from 0 to 350 mA to identify the LD power with the unit of milliwatts (mW). The linear fitting regression line is then figured out.

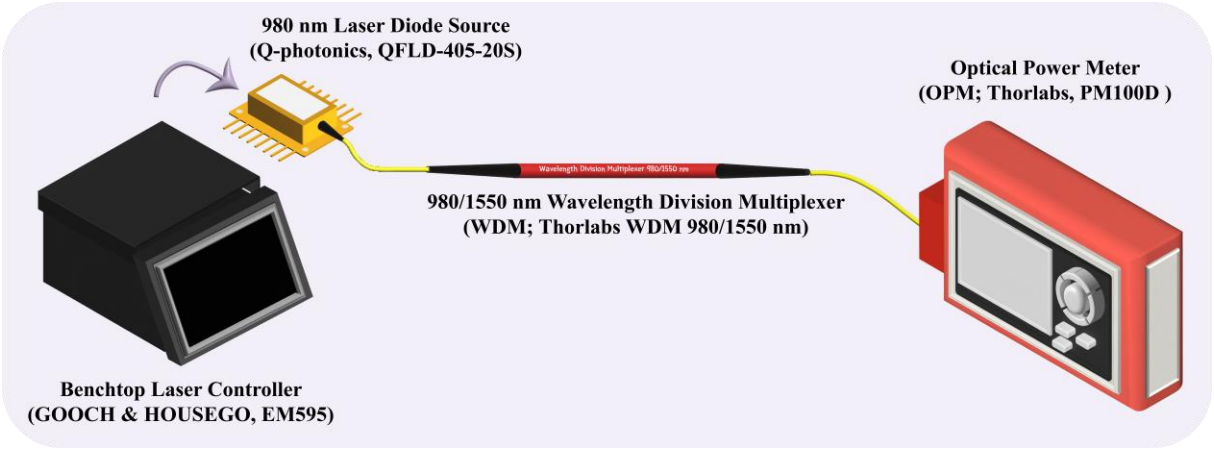

Fig. 2. Setup configuration of pump characterisation of laser diode

2.3 Passively Q-switched EDFL Ring Cavity Configuration

Figure 3 depicts the V_4AlC_3-based Q-switched EDFL ring cavity configuration. A ring cavity is preferred as the V_4AlC_3 SA is a transmissive SA [47]. For a Q-switched EDFL ring cavity design, the laser structure is mainly subdivided into three parts: the laser pumping source, the active gain medium, and the optical resonator cavity. Optical pumping, often known as LD, is a laser pumping source compatible with a fibre laser [48]. In this work, an EDF is utilised as the active gain medium in the Q-switched fibre laser configuration. Referring to the operational wavelength of EDF in the 1.5-μm region, a 980 nm LD is essential to ensure efficient power pumping towards the resonator ring cavity configuration [49].

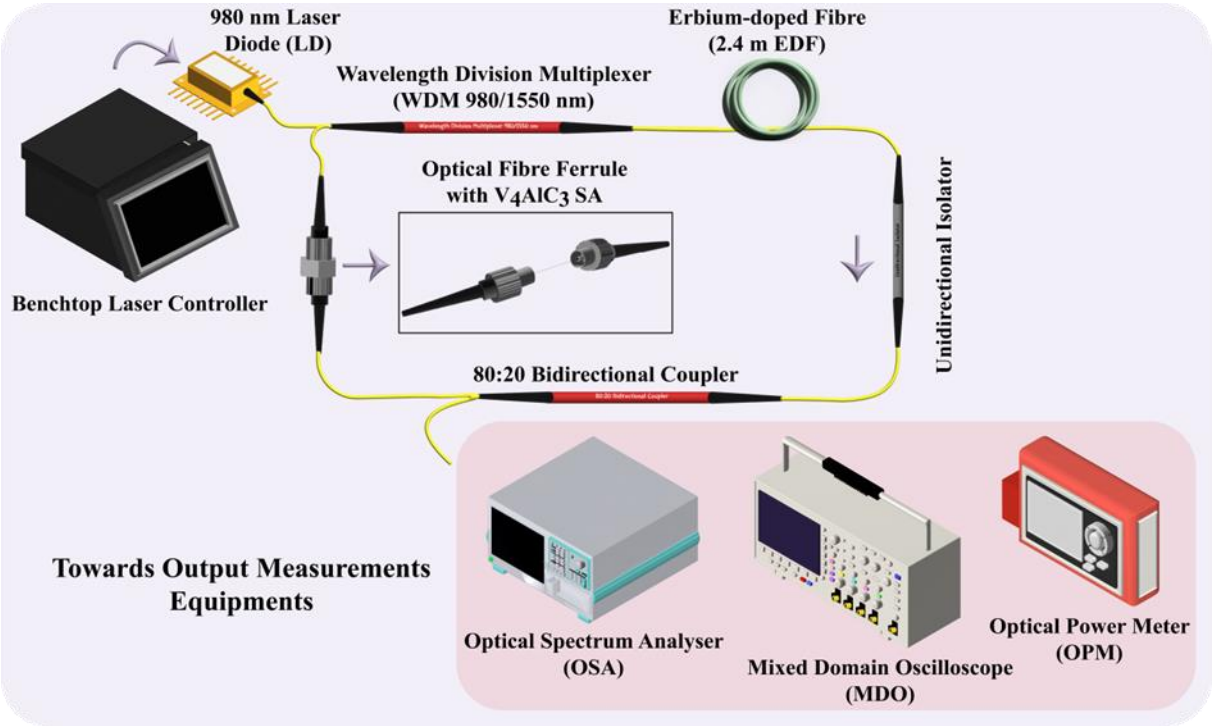

Fig. 3. V_4AlC_3 -based Q-switched EDFL ring cavity configuration

The design of the resonator ring cavity is described as follows. A WDM with a forward pumping end of 980 nm and a backward pumping end of 1550 nm is utilised to multiplex the optical signal and

interconnect between the 980 nm LD pumping source and the resonator ring cavity. A 2.4 m EDF (NUFERN, SM-ESF-7/125) with specification as mentioned in Table 1. functions as the active gain medium. It is located next to the WDM and further joined to a unidirectional polarisation-insensitive optical isolator (ISO). The ISO plays a pivotal role in ensuring one directional optical signal propagation without backflow that might cause damage towards LD.

Table 1
Specifications of the EDF

Specifications	Value
Mode field diameter (MFD)	8.8 ± 1.0 μm at 1550 nm
Cut-off wavelength	1400 ± 60 nm
Core numerical aperture	0.150
Core absorption	55.0 ± 5.0 dB/m at 1530 nm

A bidirectional coupler with a coupling ratio of 80:20 is connected next to the ISO to fractionate the optical signals. 80% of the optical signals would flow towards the optical fibre ferrule integrated with V_4AlC_3 SA and circulated to the WDM to complete the resonator ring cavity setup. Another 20% is split and distributed to the external measuring equipment. Through this Q-switched EDFL ring cavity configuration, several analyses can be done by connecting this 20% port of the bidirectional coupler to the corresponding measuring equipment.

To investigate the importance of the presence of V_4AlC_3 SA, an experiment was conducted by connecting the EDFL ring cavity configuration with and without the V_4AlC_3 SA to an optical spectrum analyser (OSA; Yokogawa, AQ6370D). The SNR value and wavelength shifting of these EDFL ring cavity configurations were observed through this demonstration. The experiment work conforms to the performance parameters of the V_4AlC_3-based Q-switched EDFL ring cavity configuration. Principally, the performance parameters of a Q-switched fibre laser correspond to the determinants that affect the modulation of the Q-factor as expressed in Eq. (1) [50].

$$Q = \frac{2\pi f_0 \varepsilon}{P} \tag{1}$$

where Q represents the Q-factor, f_0 represents the resonant frequency, ε represents the stored energy in the resonant cavity, and P represents the power dissipated. The performance parameters are classified into temporal and power-related parameters. The temporal parameters are the pulse repetition rate f_R, pulse repetition interval T_R, pulse width $\Delta\tau$, and duty cycle D. The power-related parameters are output power P_{avg}, pulse energy U and peak power P_{peak}. The temporal parameters are determined by a mixed domain oscilloscope (MDO; TEKTRONIX, MDO3024), while the power-related parameter, the output power is identified by an optical power meter (OPM; THORLABS, PM100D) and the pulse energy and peak power are investigated through the calculations as expressed in Eq. (2) and (3) [51].

$$U = \frac{P_{avg}}{f_R} = P_{avg} \cdot T_R \tag{2}$$

$$P_{peak} = 0.94 \frac{U}{\Delta\tau} = 0.94 \frac{P_{avg} \cdot T_R}{\Delta\tau} = 0.94 \frac{P_{avg}}{D} \tag{3}$$

The experiment work was conducted by increasing the pumping power along the stable LD pumping power range of the V_4AlC_3-based Q-switched EDFL ring cavity configuration. The variance of parameters was seen accompanying the growth of pump power.

3. Results and Discussion

This section discusses the results of pump characterization of laser diode, the experiment of EDFL ring cavity with and without V_4AlC_3 SA, and the performance parameters of V_4AlC_3-based Q-switched EDFL ring cavity configuration.

3.1 Pump Characterisation of Laser Diode

Figure 4 shows the pump characterisation of the laser diode. By increasing the pump power from 0 to 350 mA, the LD pump power in the unit of milliwatts was determined to initiate at 40 mA as 3.5 mW. The pump power was increased proportionately until the maximum of 177.6 mW at 350 mA. This indicated that the LD is stable from 3.5 mW to 177.6 mW. Nevertheless, a best-fitting linear regression model of the pump characterisation was investigated through the calculation as expressed in Eq. (4).

$$y = 0.56x - 18.96 \tag{4}$$

where y is the LD pump power in milliwatts while x is the LD pump power in milliamperes. This equation demonstrated the unit conversion of LD pump power from milliamperes to milliwatts.

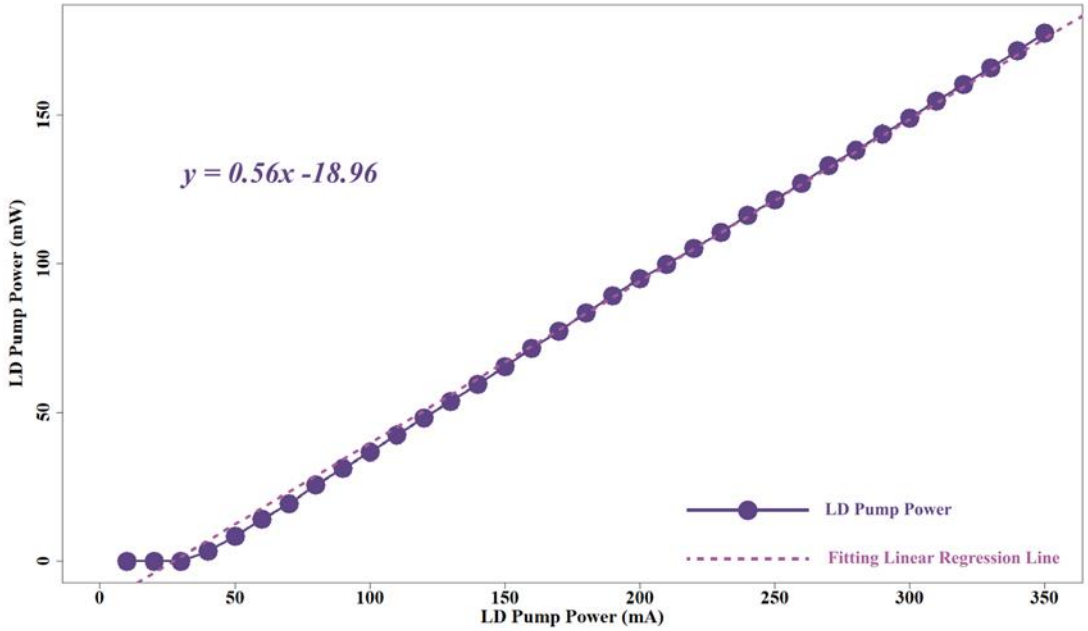

Fig. 4. Pump characterisation of laser diode

3.2 Experiment of EDFL Ring Cavity with and without V_4AlC_3 SA

Figure 5 compares the optical spectrum of EDFL ring cavity configuration with and without V_4AlC_3 SA. Before the integration of V_4AlC_3 SA into the EDFL ring cavity, the fibre laser is under a continuous wave laser operation. The stable range of this EDFL ring cavity configuration is 3.5 to 177.6 mW. The

centre wavelength λ_c is attained at 1563.50 nm while the SNR value is 47.98 dBm. The stable range is narrowed after the implementation of V_4AlC_3 SA into the EDFL configuration from 87.74 to 177.60 mW. Concurrently, the λ_c is determined to undergo a left shifting to 1560.16 nm while the SNR value is improved to 54.83 dBm.

The left shifting of λ_c of the EDFL ring cavity with V_4AlC_3 SA towards the near-infrared region can be explained by Plank's law as in Eq. (5) [50]. *E* symbolises the photon energy, *h* is Plank's constant (6.626×10^{-34} Js), *c* is the speed of light while λ defines the operational wavelength, which is also known as Q-switching wavelength respectively. As stated in Eq. (5), the photon energy possesses an inverse relationship to the Q-switching wavelength. Hence, the photon energy will increase with the decrease of the Q-switching wavelength.

$$E = h\left(\frac{c}{\lambda}\right) \tag{5}$$

The increase in SNR value is great evidence of quality betterment. This is because fewer noise signals cause relatively more optical signals to be transmitted over the EDFL ring cavity. In a nutshell, the insertion of V_4AlC_3 SA into the EDFL configuration not only generates the Q-switching pulses but also provides an outstanding improvement in terms of photon energy and SNR value.

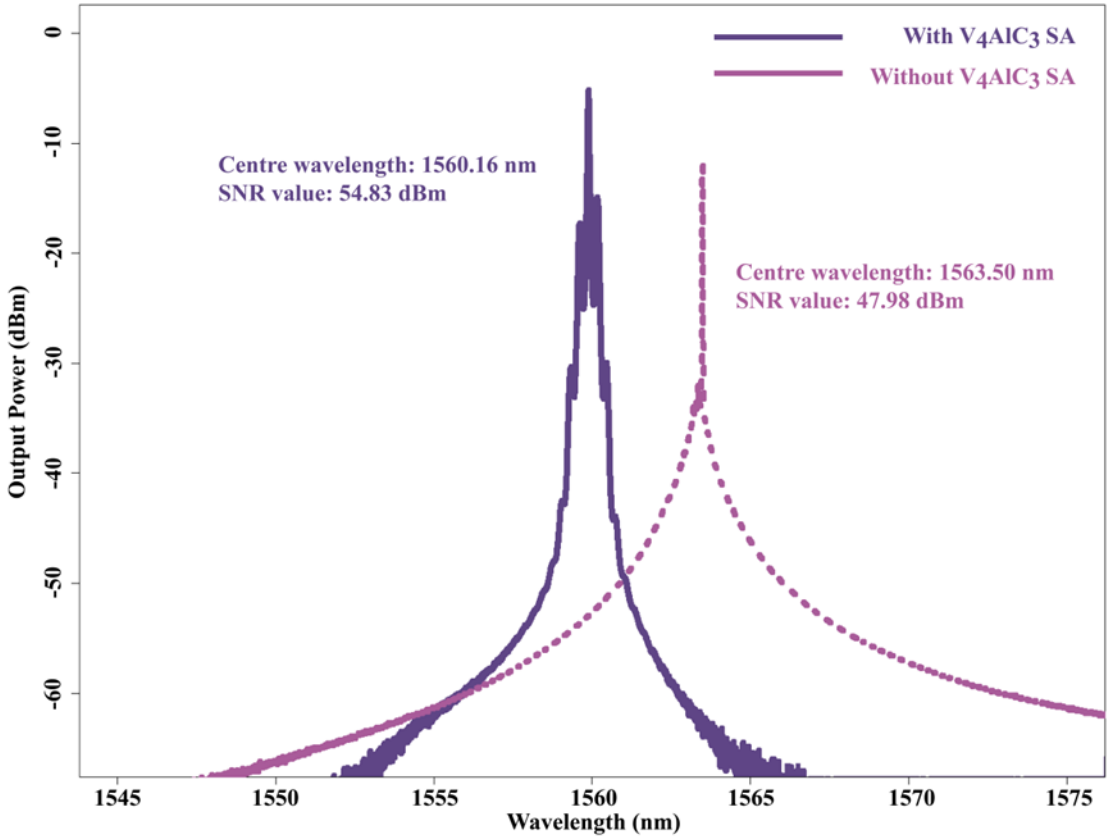

Fig. 5. Comparison of optical spectra of EDFL configuration with and without V_4AlC_3

3.3 Performance Parameters of V_4AlC_3-based Q-switched EDFL Ring Cavity Configuration

Figure 6(a) exhibits the pulse repetition rate and pulse width along with the increasing pump power of the V_4AlC_3-based Q-switched EDFL ring cavity configuration. The pulse repetition rate increased from 38.29 to 54.37 kHz with the increasing pump power from 87.74 to 177.60 mW. The

pulse repetition rate of this Q-switched EDFL ring cavity configuration increases gradually with the LD pump power [30]. In parallel with the amplifying LD pump power, the number of emitted pulses is increased, hence the pulse repetition rate is increased. The pulse width is in an inverse-proportional relationship with the pump power. Along the stable LD pump power range, the pulse width decreases from 9.06 μs to its minimum of 6.43 μs. This is appropriate as the more optical pulses emitted within an interval escorted with the augmentation of LD pump power, the narrower the pulse generated.

Next, Figure 6(b) illustrates the relationship between pulse repetition interval and duty cycle with pump power. The pulse repetition interval decreases sequentially from 26.12 to 18.33 μs. This reflects the time interval between the successive pulses as being more compressed with the increasing pump power. This leads to an increase in pulse repetition rate. Nevertheless, the pulse repetition rate is the reciprocal of the pulse repetition rate. Considering the intensifying pulse repetition rate, the pulse repetition interval is phasing down. The pulse repetition interval is determined to be approximately three times the pulse width as validated by the duty cycle which reflects the ratio of pulse width to pulse repetition interval of the V_4AlC_3-based Q-switched EDFL ring cavity configuration with an average value of around 0.326 (a.u.). This indicated that the pulse width is one-third of the pulse repetition interval.

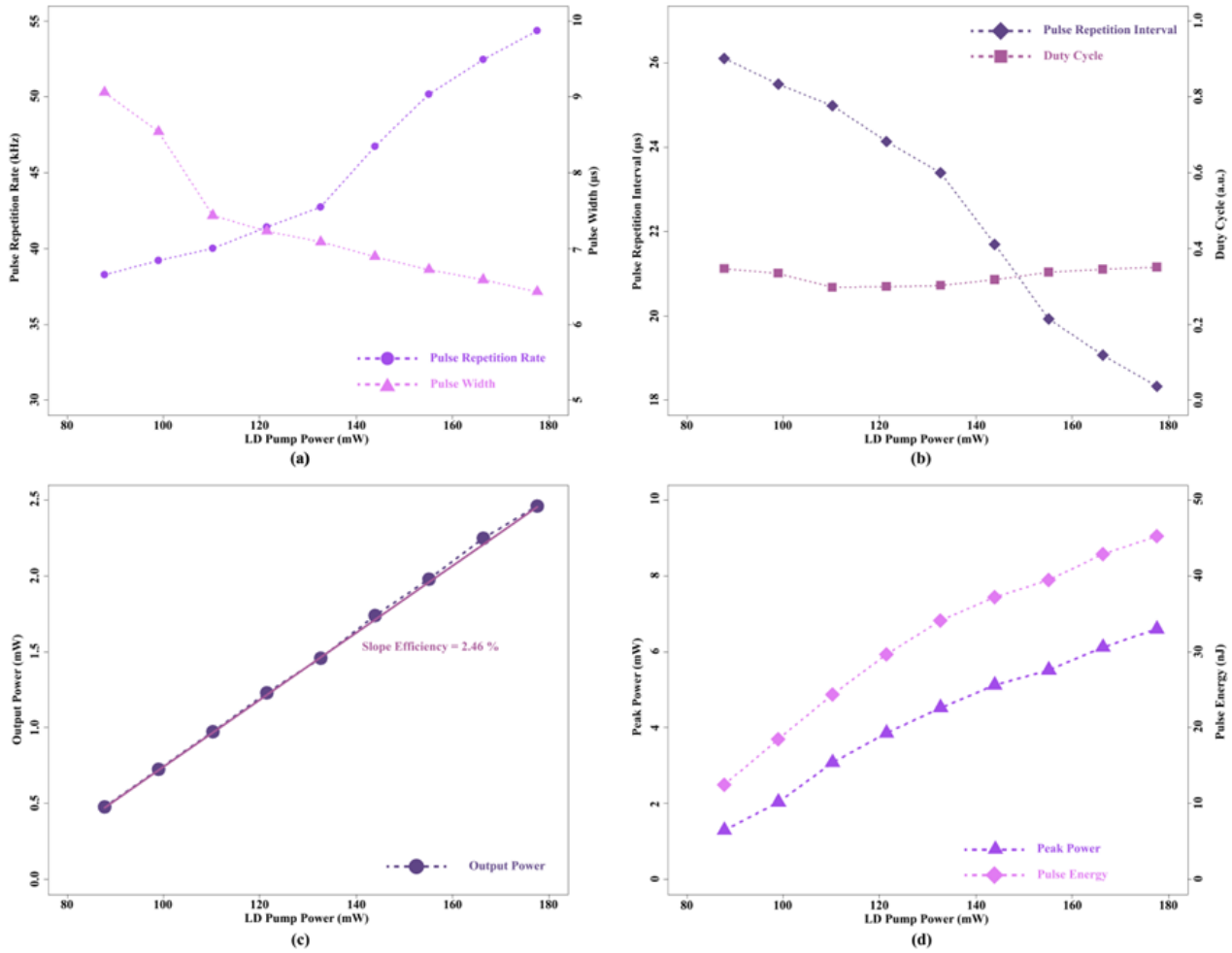

Fig. 6. (a) Pulse repetition rate and pulse width (b)pulse repetition interval and duty cycle (c) output power and (d) peak power and pulse energy against pump power

Figure 6(c) shows the output power of the V_4AlC_3-based Q-switched EDFL ring cavity configuration along with the pump power. The output power linearly increases from 0.48 mW to its maximum of

2.46 mW with a slope efficiency of 2.46 %. The higher the LD pump power, the higher the output power attained until its maximum. This result is satisfied as the output power is ideally expanded in linear regression. Figure 6(d) illustrates the peak power and pulse energy with the increasing pump power. When the pump power increases perpetually from 87.74 to 177.60 mW, the peak power also demonstrates progress from 1.293 to 6.601 mW. This means that the peak power is linearly proportionate to the pump power. Also, this outcome can be clarified by the expression in Eq. (3); i.e., peak power increases with output power, while output power increases with LD pump power. The pulse energy exhibits a forward increment from 12.458 to 45.246 nJ. The pulse energy is directly proportionate to the LD pump power. This is as described in Eq. (2), whereby pulse energy increases as an accessory to the output power at the same time as the increment of output power with the LD power.

In summary, the performance parameters with the increasing LD pump power are to the point such that a passively Q-switched fibre laser is favourable. The temporal parameters, in particular, the maximum pulse repetition rate, the minimum pulse repetition interval, the minimum pulse width, and the duty cycle is determined as 54.37 kHz, 18.33 μs, 6.43 μs, and 0.326, accordingly. The power-related parameters, in general, the maximum output power, peak power and pulse energy is indicated to be 2.5 mW, 6.602 mW and 45.246 nJ, respectively.

4. Conclusions

The V_4AlC_3 SA fabricated through solution casting has effectively performed as a Q-switcher in an EDFL ring cavity configuration. The Q-switching wavelength of this V_4AlC_3-based passively Q-switched EDFL is accomplished at 1560.16 nm. The energetic Q-switching pulse generated is determined to have the maximum pulse repetition rate, the minimum pulse repetition interval, the minimum pulse width and duty cycle of 54.37 kHz, 18.33 μs, 6.43 μs and 0.326. The maximum output power is identified as 2.5 mW, while the pulse energy and peak power are calculated to be 45.246 nJ and 6.602 mW in accordance. The experiment work signifies that V_4AlC_3 SA is appropriate to serve as a Q-switcher to generate a stable and powerful Q-switching pulse train at the 1.5-μm region. The realisation of this V_4AlC_3-based passively Q-switched EDFL has placed confidence in various disciplines, including optical communication, sensing and ranging, laser ablation, drilling and welding, medical and surgical implementation, and scientific and technological research.

Acknowledgement

This research work is funded by the Universiti Teknologi Malaysia under UTM Fundamental Research (Q.K130000.3843.22H96).

References

[1] Nesser, Manar, O. Maloberti, E. Salloum, J. Dupuy, S. Panier, C. Pineau, J-P. Birat, J. Fortin, and P. Dassonvalle. "Impact of Ultra-Short Pulsed Laser (USPL) ablation process on separated loss coefficients of grain oriented electrical steels." *IEEE Transactions on Magnetics* 58, no. 8 (2022): 1-5. https://doi.org/10.1109/TMAG.2022.3152899

[2] Yuan, Junjie, Guowei Liu, Yi Xin, Fei Xing, Kezhen Han, Wenfei Zhang, Fang Zhang, and Shenggui Fu. "Passively Q-switched modulation based on antimonene in erbium-doped fiber laser with a long term stability." *Optical Materials* 118 (2021): 111256. https://doi.org/10.1016/j.optmat.2021.111256

[3] Ahmad, Harith, Nur Atikah Azali, and Norazriena Yusoff. "Liquid phase exfoliation of hafnium diselenide and its role in initiating the mode-locked pulse laser at eye-safe wavelength region." *Optical Materials* 123 (2022): 111933. https://doi.org/10.1016/j.optmat.2021.111933

[4] Li, Maojun, Guocui Gan, Yi Zhang, and Xujing Yang. "Thermal damage of CFRP laminate in fiber laser cutting process and its impact on the mechanical behavior and strain distribution." *Archives of Civil and Mechanical Engineering* 19, no. 4 (2019): 1511-1522. https://doi.org/10.1016/j.acme.2019.08.005

[5] Kim, T. H. "Analysis of optical communications, fiber optics, sensors and laser applications." *J. Mach. Comput* 3, no. 2 (2023): 115-125. https://doi.org/10.53759/7669/jmc202303012

[6] Panda, Saran Srihari Sripada, Trilochan Panigrahi, Saidi Reddy Parne, Samrat L. Sabat, and Linga Reddy Cenkeramaddi. "Recent advances and future directions of microwave photonic radars: a review." *IEEE Sensors Journal* 21, no. 19 (2021): 21144-21158. https://doi.org/10.1109/JSEN.2021.3099533

[7] Salam, Sameer, A. H. H. Al-Masoodi, Ahmed Shakir Al-Hiti, Ab HH Al-Masoodi, Pengfei Wang, Wei Ru Wong, and Sulaiman Wadi Harun. "FIrpic thin film as saturable absorber for passively Q-switched and mode-locked erbium-doped fiber laser." *Optical fiber technology* 50 (2019): 256-262. https://doi.org/10.1016/j.yofte.2019.04.005

[8] Heiderscheit, Timothy, Ninggang Shen, Qinghua Wang, Avik Samanta, Benxin Wu, and Hongtao Ding. "Keyhole cutting of carbon fiber reinforced polymer using a long-duration nanosecond pulse laser." *Optics and Lasers in Engineering* 120 (2019): 101-109. https://doi.org/10.1016/j.optlaseng.2019.03.009

[9] Sun, Zhipei, Daniel Popa, Tawfique Hasan, Felice Torrisi, Fengqiu Wang, Edmund JR Kelleher, John C. Travers, Valeria Nicolosi, and Andrea C. Ferrari. "A stable, wideband tunable, near transform-limited, graphene-mode-locked, ultrafast laser." *Nano Research* 3 (2010): 653-660. https://doi.org/10.1007/s12274-010-0026-4

[10] Sun, Guoqing, Ming Feng, Kang Zhang, Tianhao Wang, Yuanhao Li, Dongdong Han, Yigang Li, and Feng Song. "Q-Switched and Mode-Locked Er-doped fiber laser based on MAX phase Ti2AlC saturable absorber." *Results in physics* 26 (2021): 104451. https://doi.org/10.1016/j.rinp.2021.104451

[11] Ahmad, Harith, Rizal Ramli, Nor Najwa Ismail, Siti Nabila Aidit, Norazriena Yusoff, and Muhamad Zharif Samion. "Passively mode locked thulium and thulium/holmium doped fiber lasers using MXene Nb2C coated microfiber." *Scientific reports* 11, no. 1 (2021): 11652. https://doi.org/10.1038/s41598-021-90978-x

[12] Peng, Xi, and Yixin Yan. "Graphene saturable absorbers applications in fiber lasers." *Journal of the European Optical Society-Rapid Publications* 17, no. 1 (2021): 16. https://doi.org/10.1186/s41476-021-00163-w

[13] Ma, Chunyang, Cong Wang, Bo Gao, Jordan Adams, Ge Wu, and Han Zhang. "Recent progress in ultrafast lasers based on 2D materials as a saturable absorber." *Applied Physics Reviews* 6, no. 4 (2019). https://doi.org/10.1063/1.5099188

[14] Liu, Wenjun, Mengli Liu, Ximei Liu, Xiaoting Wang, Hui-Xiong Deng, Ming Lei, Zhongming Wei, and Zhiyi Wei. "Recent advances of 2D materials in nonlinear photonics and fiber lasers." *Advanced Optical Materials* 8, no. 8 (2020): 1901631. https://doi.org/10.1002/adom.201901631

[15] Woodward, Robert I., and Edmund JR Kelleher. "2D saturable absorbers for fibre lasers." *Applied Sciences* 5, no. 4 (2015): 1440-1456. https://doi.org/10.3390/app5041440

[16] Ridha, Fay F., Abdul Hadi Al-Janabi, and Ali H. Abdalhadi. "Self-starting Q-switched pulse generation in EDFL ring cavity based on Ta2AlC MAX-phase saturable absorber." *Infrared Physics & Technology* 123 (2022): 104183. https://doi.org/10.1016/j.infrared.2022.104183

[17] Zhu, Rui, Yaoyao Qi, and Jianfei Meng. "Novel nanomaterials based saturable absorbers for passive mode locked fiber laser at 1.5 μm." *Nanotechnology* 33, no. 18 (2022): 182002. https://doi.org/10.1088/1361-6528/ac4d59

[18] Debnath, Pulak Chandra, and Dong-Il Yeom. "Ultrafast fiber lasers with low-dimensional saturable absorbers: status and prospects." *Sensors* 21, no. 11 (2021): 3676. https://doi.org/10.3390/s21113676

[19] Zhang, Baitao, Jun Liu, Cong Wang, Kejian Yang, Chaokuei Lee, Han Zhang, and Jingliang He. "Recent progress in 2D material-based saturable absorbers for all solid-state pulsed bulk lasers." *Laser & Photonics Reviews* 14, no. 2 (2020): 1900240. https://doi.org/10.1002/lpor.201900240

[20] Nizamani, Bilal, Faisal Ahmed Memon, Zeshan Adeel Umar, Sameer Salam, Mustafa Mohammed Najm, MIM Abdul Khudus, Effariza Hanafi, Muhammed Aslam Baig, and Sulaiman Wadi Harun. "Q-switched erbium-doped fiber laser with silicon oxycarbide saturable absorber." *Optik* 219 (2020): 165234. https://doi.org/10.1016/j.ijleo.2020.165234

[21] Gulyamov, G., U. I. Erkaboev, N. A. Sayidov, and R. G. Rakhimov. "The influence of temperature on magnetic quantum effects in semiconductor structures." *Journal of Applied Science and Engineering* 23, no. 3 (2020): 453-460. http://jase.tku.edu.tw/articles/jase-202009-23-3-0009

[22] Diblawe, Abdulkadir Mukhtar, Mustafa Mohammed Najm, Bilal Nizamani, Ahmad Haziq Aiman Rosol, Abdullahi Mohamed Samatar, Kaharudin Dimyati, Moh Yasin, Zian Cheak Tiu, and Sulaiman Wadi Harun. "Q-switched fiber laser in C-band region using metal ceramic-based saturable absorber." *Optik* 264 (2022): 169395. https://doi.org/10.1016/j.ijleo.2022.169395

[23] Rao, Soma Venugopal, K Naga Krishnakanth, C Indumathi, and TC Sabari Girisun. "Non-Linear Optical Properties of Novel Nanomaterials." *Handbook of Laser Technology and Applications: Lasers Applications: Materials Processing and Spectroscopy (Volume Three)* 3 (2021): 255. https://doi.org/10.1201/9781315310855-21

[24] Bao, Qiaoliang, Han Zhang, Yu Wang, Zhenhua Ni, Yongli Yan, Ze Xiang Shen, Kian Ping Loh, and Ding Yuan Tang. "Atomic-layer graphene as a saturable absorber for ultrafast pulsed lasers." *Advanced Functional Materials* 19, no. 19 (2009): 3077-3083. https://doi.org/10.1002/adfm.200901007

[25] Haris, H., S. W. Harun, A. R. Muhammad, C. L. Anyi, S. J. Tan, F. Ahmad, R. M. Nor, N. R. Zulkepely, and H. Arof. "Passively Q-switched Erbium-doped and Ytterbium-doped fibre lasers with topological insulator bismuth selenide (Bi2Se3) as saturable absorber." *Optics & laser technology* 88 (2017): 121-127. https://doi.org/10.1016/j.optlastec.2016.09.015

[26] Ahmad, Harith, Nor Hidayah Abdul Kahar, Norazriena Yusoff, Muhamad Zharif Samion, Siti Aisyah Reduan, Mohammad Faizal Ismail, Leonard Bayang, Yu Wang, Siyi Wang, and Jayanta K. Sahu. "Passively Q-switched 1.3 µm bismuth doped-fiber laser based on transition metal dichalcogenides saturable absorbers." *Optical Fiber Technology* 69 (2022): 102851. https://doi.org/10.1016/j.yofte.2022.102851

[27] Wang, Junli, Yupeng Xing, Lei Chen, Sha Li, Haotian Jia, Jiangfeng Zhu, and Zhiyi Wei. "Passively Q-switched Yb-doped all-fiber laser with a black phosphorus saturable absorber." *Journal of Lightwave Technology* 36, no. 10 (2018): 2010-2016. https://doi.org/10.1109/JLT.2018.2800910

[28] Chen, Hongling, Mao Zhou, Peixiong Zhang, Hao Yin, Siqi Zhu, Zhen Li, and Zhenqiang Chen. "Passively Q-switched Nd: GYAP laser at 1.3 µm with bismuthene nanosheets as a saturable absorber." *Infrared Physics & Technology* 121 (2022): 104023. https://doi.org/10.1016/j.infrared.2022.104023

[29] Ahmad, Harith, A. A. Kamely, M. K. A. Zaini, M. Z. Samion, W. Y. Chong, A. K. Zamzuri, and K. S. Lim. "Generation of four-wave mixing with nonlinear Vanadium-carbide (V2C)-deposited side-polished fiber (SPF) in 1.5-and 2.0-µm wavelength operation." *Optics & Laser Technology* 145 (2022): 107458. https://doi.org/10.1016/j.optlastec.2021.107458

[30] Jafry, Afiq Arif Aminuddin, Nabilah Kasim, Bilal Nizamani, Ahmad Razif Muhammad, Sulaiman Wadi Harun, and Preecha Yupapin. "MAX phase Ti3AlC2 embedded in PVA and deposited onto D-shaped fiber as a passive Q-switcher for erbium-doped fiber laser." *Optik* 224 (2020): 165682. https://doi.org/10.1016/j.ijleo.2020.165682

[31] Najm, M. M., B. Nizamani, P. Zhang, H. Arof, A. S. Al-Hiti, A. H. A. Rosol, M. C. Paul, M. Yasin, and S. W. Harun. "Chromium aluminum carbide as Q-switcher for the near-infrared erbium-doped fiber laser." *Optik* 250 (2022): 168362. https://doi.org/10.1016/j.ijleo.2021.168362

[32] Al-Masoodi, Ahmed HH, Fauzan Ahmad, Mahmoud HM Ahmed, Hamzah Arof, and Sulaiman W. Harun. "Q-switched ytterbium-doped fiber laser with topological insulator-based saturable absorber." *Optical Engineering* 56, no. 5 (2017): 056103-056103. https://doi.org/10.1117/1.OE.56.5.056103

[33] Ahmad, Harith, N. Sadafi, N. Yusoff, M. Z. Samion, M. F. Ismail, and W. Y. Chong. "Arc-shaped fiber coated with Ta2AlC MAX phase as mode-locker for pulse laser generation in thulium/holmium doped fiber laser." *Optik* 252 (2022): 168508. https://doi.org/10.1016/j.ijleo.2021.168508

[34] Mao, Dong, Mingkun Li, Xiaoqi Cui, Wending Zhang, Hua Lu, Kun Song, and Jianlin Zhao. "Stable high-power saturable absorber based on polymer-black-phosphorus films." *Optics Communications* 406 (2018): 254-259. https://doi.org/10.1016/j.optcom.2016.11.027

[35] Pumera, Martin, and Zdeněk Sofer. "2D monoelemental arsenene, antimonene, and bismuthene: beyond black phosphorus." *Advanced Materials* 29, no. 21 (2017): 1605299. https://doi.org/10.1002/adma.201605299

[36] Jhon, Young In, Joonhoi Koo, Babak Anasori, Minah Seo, Ju Han Lee, Yury Gogotsi, and Young Min Jhon. "Metallic MXene saturable absorber for femtosecond mode-locked lasers." *Advanced Materials* 29, no. 40 (2017): 1702496. https://doi.org/10.1002/adma.201702496

[37] Tuo, Mingfen, Chuan Xu, Haoran Mu, Xiaozhi Bao, Yingwei Wang, Si Xiao, Weiliang Ma et al. "Ultrathin 2D transition metal carbides for ultrafast pulsed fiber lasers." *Acs Photonics* 5, no. 5 (2018): 1808-1816. https://doi.org/10.1021/acsphotonics.7b01428

[38] Feng, Xiao-Yue, Bao-Yong Ding, Wei-Yuan Liang, Feng Zhang, Ting-Yin Ning, Jie Liu, and Han Zhang. "MXene Ti3C2Tx absorber for a 1.06 µm passively Q-switched ceramic laser." *Laser Physics Letters* 15, no. 8 (2018): 085805. https://doi.org/10.1088/1612-202X/aac91d

[39] Lee, Kyungtaek, Suh-young Kwon, Taeho Woo, Janghyun Ryu, Junha Jung, and Ju Han Lee. "Nonlinear absorption and refraction properties of V4C3 MXene and its use for an ultra-broadband saturable absorber." *Advanced Optical Materials* 11, no. 13 (2023): 2300213. https://doi.org/10.1002/adom.202300213

[40] Qin, Tianchen, Zegao Wang, Yuqing Wang, Flemming Besenbacher, Michal Otyepka, and Mingdong Dong. "Recent progress in emerging two-dimensional transition metal carbides." *Nano-Micro Letters* 13, no. 1 (2021): 183. https://doi.org/10.1007/s40820-021-00710-7

[41] Guo, Yitong, Sen Jin, Libo Wang, Pingge He, Qianku Hu, Li-Zhen Fan, and Aiguo Zhou. "Synthesis of two-dimensional carbide Mo2CTx MXene by hydrothermal etching with fluorides and its thermal stability." *Ceramics International* 46, no. 11 (2020): 19550-19556. https://doi.org/10.1016/j.ceramint.2020.05.008

[42] Ahmad, Harith, Hissah Saedoon M. Albaqawi, Norazriena Yusoff, Wu Yi Chong, and Moh Yasin. "Q-Switched Fiber Laser at $1.5~\mu $ m Region Using Ti 3 AlC 2 MAX Phase-Based Saturable Absorber." *IEEE journal of quantum electronics* 56, no. 2 (2019): 1-6. https://doi.org/10.1109/JQE.2019.2949798

[43] Lee, Jinho, Suhyoung Kwon, and Ju Han Lee. "Ti 2 AlC-based saturable absorber for passive Q-switching of a fiber laser." *Optical materials express* 9, no. 5 (2019): 2057-2066. https://doi.org/10.1364/OME.9.002057

[44] Rudko, G. Yu, A. O. Kovalchuk, V. I. Fediv, Q. Ren, W. M. Chen, I. A. Buyanova, and Galia Pozina. "Role of the host polymer matrix in light emission processes in nano-CdS/poly vinyl alcohol composite." *Thin Solid Films* 543 (2013): 11-15. https://doi.org/10.1016/j.tsf.2013.04.035

[45] Anuar, Shairazi Akmal, Mohd Fauzi Ab Rahman, Amal Muaz Nasir, Anas Abdul Latiff, and Afiq Arif Aminuddin Jafry. "Q-switched erbium-doped fiber laser generation using titanium aluminum carbonitride Ti3Al (C0. 5N0. 5) 2 saturable absorber." *Journal of Advanced Research in Applied Sciences and Engineering Technology* 31, no. 1 (2023): 144-155. https://doi.org/10.37934/araset.31.1.144155

[46] Ahmad, Harith, A. A. Kamely, Norazriena Yusoff, Leonard Bayang, and Muhamad Zharif Samion. "Generation of Q-switched pulses in thulium-doped and thulium/holmium-co-doped fiber lasers using MAX phase (Ti3AlC2)." *Scientific reports* 10, no. 1 (2020): 9233.htt ps://doi.org/10.1038/s41598-020-66141-3

[47] Lau, Kuen Yao, Xiaofeng Liu, and Jianrong Qiu. "A comparison for saturable absorbers: Carbon nanotube versus graphene." *Advanced Photonics Research* 3, no. 10 (2022): 2200023. https://doi.org/10.1002/adpr.202200023

[48] Baharom, M. F., M. F. A. Rahman, A. A. Latiff, P. Wang, and S. W. Harun. "Lutetium (III) oxide film as passive mode locker device for erbium-doped fibre laser cavity." *Optics Communications* 446 (2019): 51-55. https://doi.org/10.1016/j.optcom.2019.04.047

[49] Shakaty, Aseel A., Jassim K. Hmood, Bushra R. Mahdi, R. I. Mahdi, and Alabbas A. Al-Azzawi. "Q-switched erbium-doped fiber laser based on nanodiamond saturable absorber." *Optics & Laser Technology* 146 (2022): 107569. https://doi.org/10.1016/j.optlastec.2021.107569

[50] Ling, Ooi Wei, Azura Hamzah, Norliza Mohamed, and Mahroof Mohamed Mafroos. "Performance Analysis of Passively Q-switched Fibre Laser by SWCNT-PVA Saturable Absorber." In *2022 4th International Conference on Smart Sensors and Application (ICSSA)*, pp. 34-38. IEEE, 2022. https://doi.org/10.1109/ICSSA54161.2022.9870949

[51] Ooi, Wei Ling, Azura Hamzah, Kawther M. Mustafa, Ahmad Haziq Aiman Rosol, Norliza Mohamed, Nur Najahatul Huda Saris, and Sulaiman Wadi Harun. "Molybdenum gallium carbide saturable absorber as Q-switcher in an erbium-doped fibre laser." *Optical Fiber Technology* 82 (2024): 103612. https://doi.org/10.1016/j.yofte.2023.103612